Controlling a Human–Computer Interface System With a Novel Classification Method that Uses Electrooculography Signals

Shang-Lin Wu†, Lun-De Liao†, *Member, IEEE*, Shao-Wei Lu, Wei-Ling Jiang, Shi-An Chen, *Member, IEEE*, and Chin-Teng Lin*, *Fellow, IEEE*

***Abstract*—Electrooculography (EOG) signals can be used to control human–computer interface (HCI) systems, if properly classified. The ability to measure and process these signals may help HCI users to overcome many of the physical limitations and inconveniences in daily life. However, there are currently no effective multidirectional classification methods for monitoring eye movements. Here, we describe a classification method used in a wireless EOG-based HCI device for detecting eye movements in eight directions. This device includes wireless EOG signal acquisition components, wet electrodes and an EOG signal classification algorithm. The EOG classification algorithm is based on extracting features from the electrical signals corresponding to eight directions of eye movement (up, down, left, right, up-left, down-left, up-right, and down-right) and blinking. The recognition and processing of these eight different features were achieved in real-life conditions, demonstrating that this device can reliably measure the features of EOG signals. This system and its classification procedure provide an effective method for identifying eye movements. Additionally, it may be applied to study eye functions in real-life conditions in the near future.**

***Index Terms*—Biosignal processing, classification methods, electrooculography (EOG), eye movement detection, human–computer interface (HCI).**

Manuscript received October 6, 2012; revised January 22, 2013; accepted February 13, 2013. Date of publication February 21, 2013; date of current version July 13, 2013. This work was supported in part by the UST-UCSD International Center of Excellence in Advanced Bio-engineering sponsored by the Taiwan National Science Council I-RiCE Program under Grant Number: NSC-101-2911-I-009-101, in part by NSC-101-2220-E-009-057, in part by the Aiming for the Top University Plan, under Contract 102W963, and in part by the Army Research Laboratory: 99C205. †L.-D. Liao and S.-L. Wu contributed equally to this work. *Asterisk indicates corresponding author*.

S.-L. Wu and S.-W. Lu are with the Institute of Electrical Control Engineering, National Chiao Tung University, Hsinchu 300, Taiwan (e-mail: shanglinwu.ece00g@nctu.edu.tw; swlucifer@mail.nctu.edu.tw).

L.-D. Liao is with the Singapore Institute for Neurotechnology (SINAPSE), National University of Singapore, Singapore 119615, Singapore (e-mail: gs336.tw@gmail.com).

W.-L. Jiang is with the Institute of Imaging and Biomedical Photonics, National Chiao Tung University, Tainan 711, Taiwan (e-mail: issacreal@gmail.com).

S.-A. Chen is with the Brain Research Center, National Chiao Tung University, Hsinchu 300, Taiwan (e-mail: sachen@nctu.edu.tw).

*C.-T. Lin is with the Brain Research Center and the Institute of Electrical Control Engineering, National Chiao Tung University, Hsinchu 300, Taiwan (e-mail: ctlin@mail.nctu.edu.tw).

Color versions of one or more of the figures in this paper are available online at http://ieeexplore.ieee.org.

Digital Object Identifier 10.1109/TBME.2013.2248154

I. Introduction

COMMUNICATION with the outside world is essential for the well-being of individuals with severe nervous system injuries or disorders. To achieve this communication, it is often necessary to process electrical signals that are obtained from the intact segments of the nervous system via human–computer interface (HCI) systems. For instance, amyotrophic lateral sclerosis (ALS) [1], [2] deprives patients of their ability to speak and to move their extremities. However, their eye movement functions remain relatively intact. Eye movements can be used as signals, transferring information from users to HCI systems. For example, in a feedback system, users can select a response by fixing their gaze on it for a certain amount of time without the need for a manual mouse or keyboard entry. This eye movement recognition ability reduces the time required to generate a message or command and facilitates a more natural interaction for the user. Another example of the importance of eye motion appears when humans communicate face to face. While talking to each other, eye movements play an important role in regulating the conversation. Therefore, integrating the analysis of eye movements into an HCI improves the ease of use and the quality of communication for users [3]. There are already many HCI systems [4], [5] that utilize eye movements, including systems of infrared oculography (IROG) [6], [7], dual Purkinje image (DPI) [8], and search coils (SCs) [9], [10]. These HCI systems are very useful for patients with severe disabilities. Unfortunately, most of the existing systems for processing eye movement signals are limited by their bulky designs, which restrict the patient's movement and are often too heavy to transport.

The electrooculography (EOG)-based [11]–[13] HCI system is one of the most useful systems for providing information about human eye activity by detecting changes in eye position. EOG signals are particularly useful for HCI systems because they are easier to detect: they have relatively large potential differences (amplitudes range between 15 and 200 μV), and their relationship to eye movements is linear (i.e., an angle of –30° to +30°). Considering these characteristics of EOG signals, it is not surprising that EOG-based HCI systems have become more popular in recent years [14]–[16]. An EOG-based system can be used to control a television [17], a wheelchair [18], or a keyboard [19]. Such a system provides both convenience and communication for disabled users, particularly when there is some physical restriction that prevents them from using other HCI

systems. Several methods have been proposed to decode the EOG signals resulting from eye movements [20]–[22]. Aungsakun *et al*. [23] used threshold analysis and time-domain features (i.e., the mean value, peak duration and peak potential value) to classify eye movements. These EOG features measure the potentials of the eye signals and decode them using an algorithm that distinguishes the different types of eye movement. In addition, spectral analysis has been a useful tool for categorizing eye movement features [24], [25]. Both time- and frequency-domain features are typically used to classify eye movements in analysis techniques such as the neural network [26] and support vector machine (SVM) [27] methods.

However, computation times and implementation complexity limit the use of algorithms that are based on pattern recognition, particularly in microcontroller devices. In a study by Deng and coworkers [28], a fuzzy distinction rule was used to classify EOG features. Using the fuzzy distinction rules, they had significant results classifying eye movements for applications in gaming control and eye tests. However, in the fuzzy distinction method, it is difficult to decide the bases for the fuzzy rules. This method also has wire limitations. Unfortunately, due to the complexity of its system architecture and its physical inconvenience, the fuzzy distinction rule is not applicable to real-life scenarios.

In this study, we describe a wireless EOG-based HCI device for detecting eye movements in eight directions. This system consists of wet electrodes, a wireless acquisition device, and a simple algorithm to classify the EOG signals. The wet electrodes provide sufficient electrical conductivity to acquire EOG signals. In comparison to other EOG-based HCI systems, our system classifies eye movements with high accuracy. In addition, the simple system design and the short computation time required for signal processing facilitates the implementation of this EOG-based interface. The specifications of this proposed system can be used to control a wheelchair, to direct a robotic arm in carrying heavy weights, or to surf the internet without a mouse or keyboard. Furthermore, wireless transmission is a more convenient method of transmitting EOG data. Therefore, our system incorporates wireless technology to make the system more mobile, enabling the use of EOG technology in daily life.

II. Materials and Methods

The fundamental components of the proposed device are shown in Fig. 1(a)–(d). These components include wet electrodes, a wireless EOG acquisition device, and locations for electrode placement. The EOG signals are measured by wet electrodes, shown in Fig. 1(a), which are connected to the EOG acquisition device by wires. Then, the EOG signals are processed by a preamplifier, analog-to-digital converter (ADC), and microcontroller unit, shown in Fig. 1(b). After their processing, the EOG signals are transmitted to a computer via Bluetooth technology. The signal measurement and processing methods are based on the placement of the electrodes, as shown in Fig. 1(c) and (d).

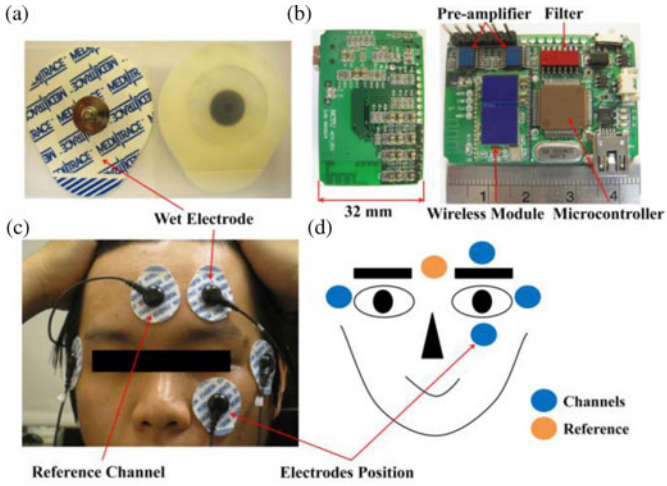

Fig. 1. Proposed EOG acquisition devices are (a) conventional wet electrodes. (b) Wireless EOG acquisition system contains a preamplifier, a filter, a microcontroller, and a wireless module. Each circuit board has a width of 32 mm. (c) Placement of each electrode followed the diagram in (d).

A. EOG Acquisition Device

The amplitudes of the EOG signals range from 15 to 200 μV, and their essential frequencies range from 0 to 30 Hz. Because EOG signals are often measured through electrodes placed around the eyes, they suffer from high noise levels that are indirectly related to eye activation. The signal artifacts in the recorded EOG are similar to those observed for electromyography (EMG) [29], [30] and electroencephalography (EEG) [31], [32] and are unessential to the experiment. The EOG acquisition device was designed to measure four channels of EOG signals, using the wet electrodes, and consists of three major units: 1) a wireless unit, 2) a preamplifier and filter unit, and 3) a microcontroller unit. The proposed wireless EOG signal acquisition device was approximately 45 $\times$ 32 $\times$ 8 mm^3 in size. A Bluetooth module was used to transmit the EOG signals wirelessly. The Bluetooth module BM0203 provided a sufficient transfer band rate (115 200 b/s) and was compliant with the computer's Bluetooth v2.0 with enhanced data rate (EDR) specification. Power was supplied by a lithium battery with an output voltage of 3 V. A commercial 750 mA·h Li-ion battery was also used to supply power to the EOG acquisition circuit, which could be continuously operated for over 12 h. The EOG signals measured by the wet electrodes were first amplified by the preamplifier unit. The preamplifier amplifies the voltage difference between the reference signals and those of the EOG electrodes while simultaneously rejecting common-mode noise (i.e., the power line noise). An instrumentation amplifier (INA2126, Texas Instruments, Dallas, TX, USA) was used for its extremely high input impedance and high common-mode rejection ratio (CMRR) ($\sim$90 dB) [33]. Instrumentation amplifiers have the ability to improve the CMRR and amplify the EOG signals to a degree that minute voltage levels can be detected. The gain of the preamplifier unit was set to 5.5 V/V. The cutoff frequency was regulated at 0.1 Hz using a high-pass filter. The

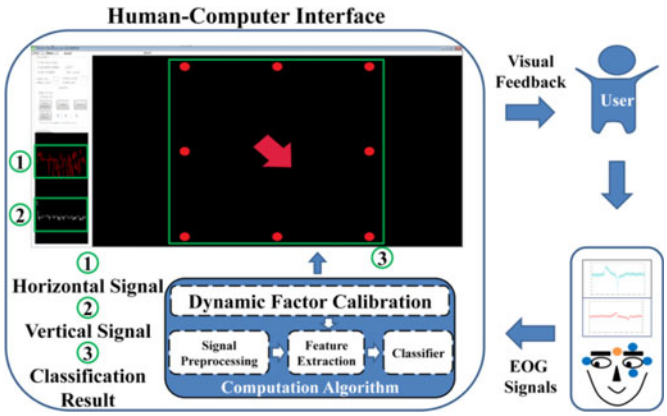

Fig. 2. Fundamental concepts for the wireless, multidirectional, EOG-based HCI system design. EOG signals are recorded by the EOG acquisition device. The signals are processed by the classification algorithm, and the results are displayed on a screen for the user.

transfer function of this preamplifier circuit was as follows:

$$\text{Gain} = A_0 + \frac{R_{\text{inner}}}{R_G + C} \tag{1}$$

$$\text{Gain} = A_0 + \frac{(sR_{\text{inner}}/R_G)}{s + (1/R_G C)}. \tag{2}$$

By using the superposition theorem reported in previous studies [34], [35], the transfer function of this preamplifier circuit can be described by (1). The values for the transfer function in (2) were the following: $R_{\text{inner}} = 80$ kΩ, $R_G = 160$ kΩ, the default value of $A_0 = 5$ V/V, and the equivalent impedance $=$ 10 μF. Equation (2) can be organized for a high-pass filter by having the resistance (R_G) and capacitance in series, with a cut-off frequency of 0.1 Hz. Therefore, the gain of the preamplifier unit was 5.5 V/V [i.e., $5 + (80 \times 10^3/160 \times 10^3)$]. In addition, the gain of the filter stage was set to 1001 V/V. Therefore, the total gain for the EOG signal acquisition device was 5505.5 V/V (5.5 $\times$ 1001 V/V). A microcontroller unit (MSP430F1611, Texas Instruments) was used to address the signal sampling rate, signal magnification, and noise reduction. The microcontroller program controlling the preamplifier and filter stage reduced the 60 Hz noise in the EOG signals using a moving average. In addition, a 12-bit resolution ADC was used to digitalize the EOG signals. The microcontroller unit was also used to digitize the EOG signals, with a sampling rate of 256 Hz. The sync filter removed signals with frequencies higher than 62.5 Hz. After removing the noise and amplifying the EOG signals, the data were transmitted to the computer interface via a wireless module.

B. Human–Computer Interface

Fig. 2 shows how the HCI communicates between the users and the computer. Before using the proposed system, the user must record their physiological parameters, which are then used to adjust the threshold value of the classification algorithm. Then, the user can begin using the eye movement detection system. First, the EOG acquisition device records the user's EOG signals. The electrode placement sites are shown in Fig. 1(c) and (d). The EOG signals are then processed using the EOG classification algorithm. Next, the processed EOG signals are transformed into eye movement results and displayed on the computer screen. Finally, the user can view the results on the screen.

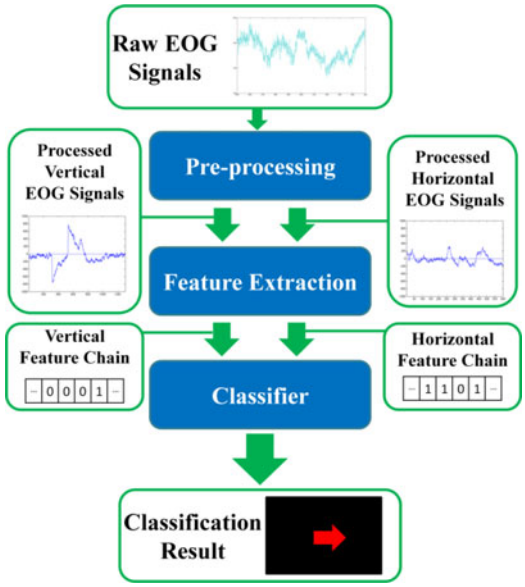

Fig. 3. Flowchart of the proposed EOG signal classification method. Raw EOG signals are processed into vertical and horizontal signals. After feature extraction and classification, the eye movement results are shown on the screen.

C. EOG Signal Classification Algorithm

The primary EOG signal analyzing method was built into the operation platform. This algorithm was composed of three parts: signal preprocessing, feature extraction, and classification (see Fig. 3). Fig. 3 shows a flowchart of the EOG signal classification method. EOG signals are processed and then separated into vertical and horizontal signals. The features are extracted, and the vertical and horizontal EOG signals are transformed into a series of features, called a feature chain. Finally, the classifier determines the eye movement indicated by the feature chain and shows the results on the screen.

1) Normalization Factor Calibration: The wireless EOG acquisition device was used to measure the eye movement activity of each user. Eye movement data were retrieved by the feature extraction function, and the eye movement activity was divided into two parts. The variation caused by the user that could change use to use corresponded to the intrasubject variation, and the eye usage habits of the user corresponded to the intersubject variation. All of the EOG features differed between each user. If the proposed system used only standard value for the features, it might not be suitable for everyone. The classification results would be worse than with the proposed option of individual calibration. The factor calibration measures the biopotential of each user's eyes, while the user makes eight types of eye movements. According to the biopotential values for those eight features, the threshold setting is optimized in the program automatically. Therefore, the calibration function was designed to resolve the intersubject variation problem. Calibration testing was composed of four trials, each of which was

executed twice. At the beginning of the trial, a red dot appears at the middle of the liquid crystal display (LCD) screen, and the users are instructed to stare at that point and follow it with their eyes. After 2 s, the red point moves to a new position temporarily (either up, down, left, right, up-left, down-left, up-right, or down-right). After 1 s, the red point returns to the initial position at the center of the screen. Users are asked to perform each type of movement twice. After the eight different directional movements have been executed, the factor calibration algorithm computes the data characteristics, including the mean and standard deviation values of the positive peak amplitude, the negative peak amplitude, the rise time, and the peak level time. These calculated characteristics are then used to adjust the classification parameters. This normalization process overcomes the intersubject variation problem so that suitable classification parameters can be determined for each user.

2) EOG Signal Preprocessing: The EOG signals, which included both vertical and horizontal signals, were recorded by the EOG acquisition device. Eye movements are always accompanied by EMG signals, which can be collected from observing the face and used to compensate for common mode noise. We assumed that EMG was the only source of noise and was constant across all electrodes. The noise caused by EMG signals can be expressed as $n(t)$, where t represents time (seconds). Additionally, we assume that the noise is independent of the electrodes and that the actual EOG signals can be expressed as a vertical EOG signal $(E_1(t))$ and a horizontal EOG signal $(E_2(t))$, which are continuous functions that change with time t (seconds). The signals are recorded by the proposed acquisition device and can be expressed as $X_1(t)$ and $X_2(t)$, where t represents time (seconds). These parameters can be related using the following equations:

$$X_1(t) = E_1(t) + n(t) \tag{3}$$

$$X_2(t) = E_2(t) + n(t). \tag{4}$$

Common-mode noise [36] was removed by subtracting (4) from (3), yielding the following equations:

$$X_1(t) - X_2(t) = E_1(t) + n(t) - E_2(t) - n(t) \tag{5}$$

$$X_1(t) - X_2(t) = E_1(t) - E_2(t). \tag{6}$$

Equation (6) describes the EOG signals after removing the EMG noise. A moving average was also used to remove redundant signals. The recorded signals are easily interfered with by 60 Hz noise, particularly when the acquisition circuit is close to electric appliances. We found that filtering using a moving average with a five-point moving window could effectively remove power-line noise.

3) Feature Extraction: After preprocessing, the eye movement features were extracted from the EOG signals. First, the preprocessed EOG signals were downsampled from 256 to 51.2 Hz to reduce the computational complexity. The signals were then individually encoded with a value sequence ranging from –2 to +2. These values were determined from the signal voltage of the EOG feature. Calibration values were used with a standard database to define four voltage thresholds, ±Th1 and ±Th2, which are used to digitalize the potential voltage. When the measured potential voltage is higher than Th2, it would be set to a digital value of 2. Potential voltages in ranges of Th1 to Th2, Th1 to –Th1, –Th1 to –Th2, and lower than –Th2 are coded to digital values of 1, 0, –1, and –2, respectively. Using the voltage parameters, the EOG signals would be converted into a sequence of values and compared to the EOG feature database (see Table I). Finally, the EOG feature sequence was transferred to the classifier to classify the eye movement.

4) EOG Signal Classifiers: The EOG signal features contain vertical and horizontal feature chains [26]. These chains were processed separately with different condition detection units, as shown in Fig. 4. Briefly, the program searches the database to conform target eye movement patterns to the feature chain. The database that we used was compiled from numerous experiments

TABLE I
DATABASE OF CODED DIGITAL SIGNALS FOR THE EIGHT EYE MOVEMENT DIRECTIONS

Directions \ Digital Value	Vertical Sequence	Horizontal Sequence
Up	0121(-1)(-2)(-1)	0000000
Down	0(-1)(-2)(-1)121	0000000
Left	0000000	0(-1)(-2)(-1)121
Right	0000000	0121(-1)(-2)(-1)
Up-right	0121(-1)(-2)(-1)	0121(-1)(-2)(-1)
Up-left	0121(-1)(-2)(-1)	0(-1)(-2)(-1)121
Down-right	0(-1)(-2)(-1)121	0121(-1)(-2)(-1)
Down-left	0(-1)(-2)(-1)121	0(-1)(-2)(-1)121

The vertical and horizontal EOG signals are coded with the digital values 0, ±1, and ±2, which are based on four thresholds: ±Th1 and ±Th2. These thresholds are used to digitalize the potential voltage. The five potential voltage ranges—higher than Th2, Th1 to Th2, Th1 to –Th1, –Th1 to –Th2 and lower than –Th2—were coded to 2, 1, 0, –1, and –2, respectively.

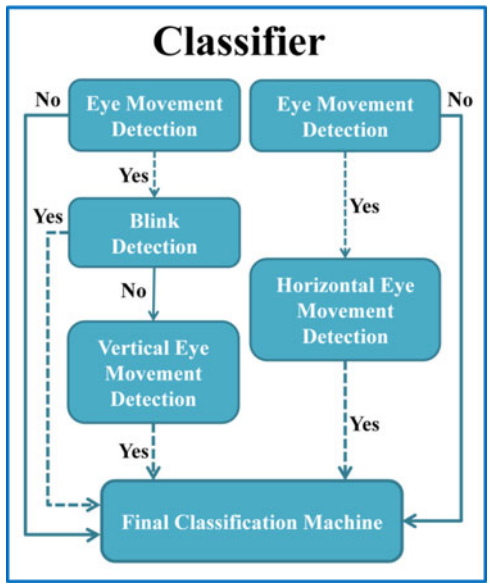

Fig. 4. EOG signal features are classified into vertical and horizontal feature chains. These chains are processed separately by different condition detection units, including vertical and horizontal eye movement detection, blink detection, and a final classification of the EOG feature.

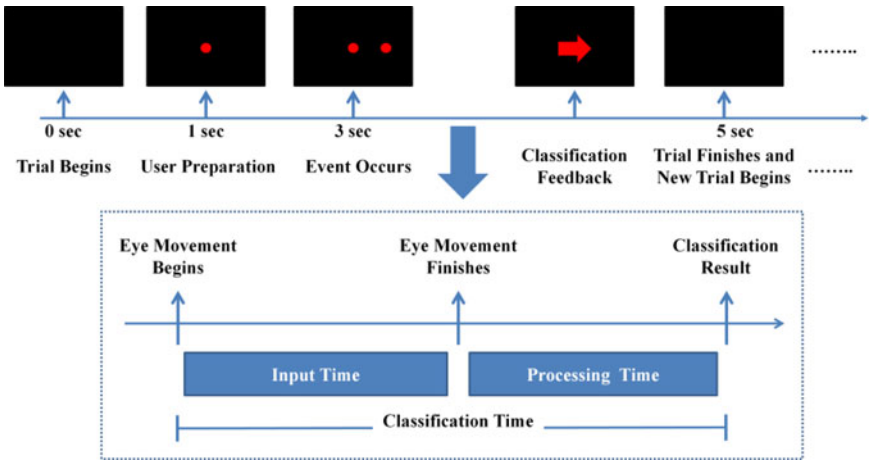

Fig. 5. Experimental trial for the task of eye movement detection shows the initial condition and the classification feedback.

and contained the eight eye movement features (up, down, left, right, up-left, down-left, up-right, and down-right). The coded EOG sequence was compared to the database. If the condition detection unit recognized the target pattern (i.e., vertical or horizontal eye movement) in the feature chain, it outputted a value of true to the final classification unit. The EOG encoding sequence was then compared to the EOG feature database, shown in Table I, and the eye movement direction that was read by the HCI was shown on the screen. If there were no patterns found in the database to match the detected sequence, the condition detection unit would output null signals and pass the feature chain to the next unit until the final classification unit was reached. By encoding the EOG signals, the eye movement characteristics can be analyzed easily.

III. Results and Discussion

Eight male users, aged 22–25 years, took part in the EOG signal measurement experiment. All of them are neurologically healthy and have corrected to normal vision. Before the experiment, the users were asked to fill out an informed consent form. Users were seated comfortably in front of a monitor and the task was explained to the participants by written instructions on the screen. Five wet electrodes were used (four channels to record the EOG signals and one for reference) to measure their EOG signals. The eye movement experiment consisted of three parts. The first was a pretest used to calibrate the classification parameters of the proposed measurement system according to each user, with the aim of identifying each user's eye movement features. The second part was a training segment on the EOG measurement system. Each of the eight directions was tested ten times. In each training trial, a red dot in the center of the screen was the starting point. After 2 s, the users were instructed to look towards a new red dot that appeared (looking in either a normal or an oblique direction). After another 2 s, both dots disappeared, and a new trial began. Last was the actual experiment, also with ten trials per direction (looking up, down, left, right, up-left, down-left, up-right, and down-right). When the dot moved to another position, users were instructed to look in the direction of the dot. The wireless EOG acquisition device was used during EOG signal measurements.

A. Experimental Procedure

The experimental procedure for monitoring eye movements is detailed in Fig. 5. Two sets of measurements were taken: one for training and one for the eight-direction eye movement experiment. Each set of measurements contained 80 trials. Before the test begins, the experimental procedure is illustrated on the screen for the user. Once the experiment starts, there is nothing on the screen. After 1 s, a red dot appears at the center of the screen. The user is instructed to stare at this dot. Two seconds later, another red dot appears on the screen, which at which the user has been instructed to look. The position of the new dot is determined by the eye movement task being tested (up, down, left, right, etc.). The order of each event type is randomized. Both the dots disappear after another 2 s, and a new trial begins.

B. Performance of the Eye Movement Features and Movement Classification

According to the experimental results for eye movement, the EOG acquisition device can successfully measure EOG signals from five wet electrodes. We tested eight different types of EOG signals, as shown in Figs. 6 and 7. Each of the EOG signals was divided into vertical and horizontal signals. The experimental results demonstrate that the action of looking up or down corresponds to vertical movement; therefore, the vertical signals for these actions are more pronounced than the horizontal signals. The action of looking up initially generates a positive peak (i.e., direction 2), which is then accompanied by a negative peak (i.e., direction 1). The negative peak corresponds to the eye returning to the center of the screen. The action of looking down initially generates a negative peak (i.e., direction 1), which is then accompanied by a positive peak (i.e., direction 2). The actions of looking left or right correspond to horizontal movements; therefore, the horizontal signals for these actions are more obvious than the vertical signals. The actions of looking left and right displayed similar results as did looking up and down, in terms of peak values. Fig. 7 displays the other four types of EOG signals, each divided into vertical and horizontal signals. These include signals for looking up-left, up-right, down-left, and down-right. These EOG signals include both horizontal and vertical components because the diagonal eye movements are

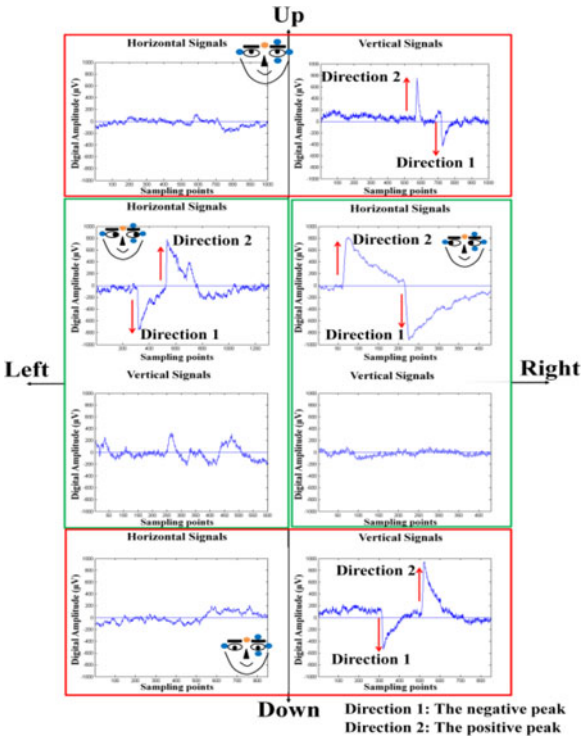

Fig. 6. Eight-direction EOG-based HCI system used wet electrodes to measure the EOG signals near the eyes. From the aforementioned experimental data, the up, down, left, and right eye motion EOG signals were effectively measured by the proposed EOG HCI system. Each EOG signal contains horizontal and vertical signals. Direction 1 represents the negative peak, and direction 2 represents the positive peak. The two signal characteristics are generated by looking in the specified direction and then returning to the center of the screen. Different eye movements have different signal characteristics (i.e., direction 1 and direction 2).

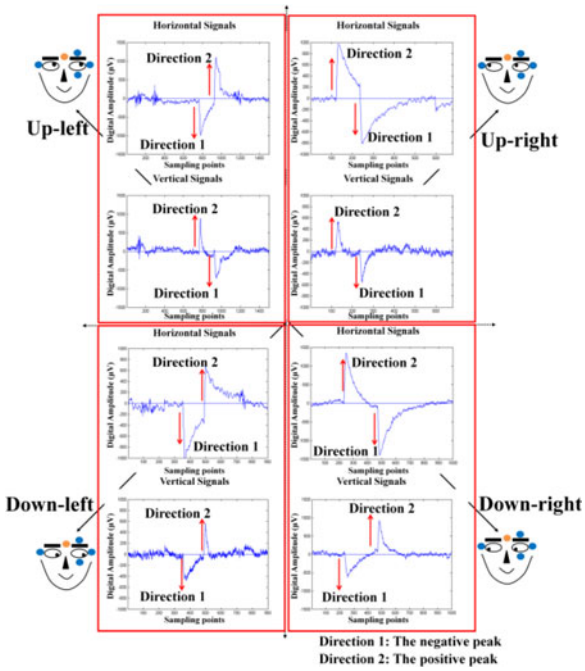

Fig. 7. Proposed multidirectional EOG-based HCI system used wet electrodes to measure the EOG signals near the eyes. From the aforementioned experimental data, the up-left, down-left, up-right, and down-right EOG signals were effectively measured by the system. Each EOG signal contains horizontal and vertical signals. Direction 1 represents the negative peak characteristic, and direction 2 represents the positive peak characteristic. The two signal characteristics are generated by looking in the specified direction and then returning to the center of the screen. Different eye movements have different signal characteristics (i.e., direction 1 and direction 2).

a combination of horizontal and vertical eye directions. The signals for these oblique movements had both positive (i.e., direction 2) and negative peaks (i.e., direction 1) in the horizontal and vertical directions. The action of looking up-left contains left and up movements; therefore, the horizontal EOG signal for looking up-left is similar to the left EOG signal, and the vertical signal is similar to the up EOG signal. Similarly, the action of looking down-left contains left and down eye movements; therefore, the horizontal EOG signal for looking down-left is similar to the left EOG signal, and the vertical signal is similar to the down EOG signal. The action of looking up-right contains right and up movements; therefore, the horizontal EOG signal for looking up-right is similar to the right EOG signal, and the vertical signal is similar to the up EOG signal. Finally, the action of looking down-right contains right and down eye movements; therefore, the horizontal EOG signal for looking down-right is similar to the looking right EOG signal, and the vertical signal is similar to the down EOG signal.

The experimental results and the accuracy of the eye movement direction classification procedure are presented in Tables II and III. Table II shows the classification accuracy of the eight-direction task. From Table II, it can be seen that some, but not all, users have difficulty with oblique directions and can be inaccurate. In addition, the standard deviations in Table II support the conclusion that the detection of normal directions is more stable than the detection of oblique directions. The highest level of accuracy obtained was 86.25%, and the average classification accuracy among the eight users was 88.59%. The most accurate type of eye movement was looking up. The system obtained a slightly higher level of accuracy when the users were looking right versus left.

TABLE II
CLASSIFICATION ACCURACIES FOR THE EIGHT TESTED EYE MOVEMENT DIRECTIONS FROM EIGHT USERS

User / Direction	S1	S2	S3	S4	S5	S6	S7	S8	Total	STD
Up	100	100	100	100	90	90	90	100	96.25	5.1755
Down	100	100	100	100	100	80	90	100	96.25	7.4402
Left	70	90	100	90	100	100	100	90	92.50	10.351
Right	90	100	90	100	90	80	80	90	90.00	7.5593
Up -right	60	90	90	80	70	100	100	80	83.75	14.0789
Up -left	80	90	100	70	60	100	80	100	85.00	15.1186
Down -right	70	100	80	50	80	90	80	80	78.75	14.5774
Down -left	80	100	100	70	90	70	90	90	86.25	11.8773
Total	81.25	96.25	95.00	82.50	85.00	88.75	88.75	91.25	88.59	

The experimental results include each user's actual average classification accuracy (%) and specific eye movement average classification accuracy (%).

TABLE III
CLASSIFICATION ACCURACY FOR EYE MOVEMENTS IS SHOWN IN THE CONFUSION MATRIX

Classification Results / Movement Directions	Up	Down	Left	Right	Up -right	Up -left	Down -right	Down -left
Up	96.7%	3.3%	0.0%	0.0%	0.0%	0.0%	0.0%	0.0%
Down	3.3%	96.7%	0.0%	0.0%	0.0%	0.0%	0.0%	0.0%
Left	6.7%	1.7%	91.7%	0.0%	0.0%	0.0%	0.0%	0.0%
Right	3.3%	0.0%	1.7%	91.7%	1.7%	1.7%	0.0%	0.0%
Up -right	13.3%	1.7%	0.0%	3.3%	81.7%	0.0%	0.0%	0.0%
Up -left	16.7%	0.0%	0.0%	0.0%	0.0%	83.3%	0.0%	0.0%
Down -right	1.7%	8.3%	0.0%	10.0%	0.0%	0.0%	78.3%	1.7%
Down -left	3.3%	6.7%	5.0%	0.0%	0.0%	0.0%	0.0%	85.0%

The experimental results presented in each row indicate the average accuracy with respect to the specific eye movement and the average accuracy with respect to the incorrect classification of other eye movements.

The measurements of noise and the user's eye movements are mitigated by using several noise removal techniques and by calibrating the experiment before measuring. The noise removal techniques used in the paper, such as high-pass filters, low-pass filters, and thresholds, were included to reduce electromagnetic interference and EMG signals. In addition, the influence of an individual user's eye movement has been solved by the calibration technique and proposed classification algorithm. Therefore, the potential influence of noise is relatively small.

1) Error of Movements in Oblique Directions: Table I show that the accuracy of oblique eye movement detection is generally lower than that of normal (i.e., up, down, left, and right) direction detection. Table III shows the accuracy obtained by users performing the eight-direction eye movement tasks. There are several possible reasons why oblique eye movements have higher levels of classification error. First, the eye movement signals resemble horizontal and vertical signals. Some of these signals are due to user mistakes during the experiments; users are tasked to perform an oblique eye movement task, but some of the users are not capable of achieving the correct eye movement. For instance, users prompted to look in the up-right direction may move their eyes up and then right, or vice versa. These user errors may be caused by personal habits or fatigue. Our results indicate that the main source of error is from the users. For example, in Table III, an up-right movement has a 13.3% chance of being classified as a looking-up action. Furthermore, a down-right eye movement has a 10% and 8.3% chance of being classified as either the looking-right or the looking-down movement, respectively. These results were obtained from the difference between the target eye movements and their classification results.

Although there is no specific error analysis in this paper, the classification results were affected by the error observed in the experiment. While examining the eye movements, unexpected motions sometimes showed up during the experiment. Misclassification typically occurred because looking up-right, looking up-left, and blinking affected the performance. Another possible reason for misclassification is a misunderstanding by the user during the calibration experiment, causing the user to perform nonstandard eye movements during the measurements.

2) Eye Movements in the Vertical Direction: Due to natural eye movement action, the measured EOG signals always include EMG signals. For vertical EOG signals, the blink EMG signals and the EOG signals generated by vertical eye movements are sometimes almost identical. Thus, in eye movement detection research, it is an important to reduce the influence of blinks. From the experimental results shown in Table II, the classification accuracy for vertical eye movements (up and down) was 96.25%, on average, because the HCI system can set a precise threshold for eye movement classification, thereby nullifying the impact of blinks on vertical EOG signals.

The EOG signal classification results shown in Table II indicate that an average classification accuracy of over 80% was obtained. Thus, the proposed eyes movement classification system resists problems associated with intersubject variation and provides a good classification method.

IV. CONCLUSION

In this study, we described a wireless EOG-based HCI for detecting eyes movements in eight directions. This system is capable of transferring EOG signals wirelessly to a computer, where the signals were processed and classified before the results were displayed to the users. The experimental results demonstrated that the proposed EOG acquisition device is able to discriminate between various movement types (looking up, looking down, etc.) and the signal characteristics associated with them. Compared with other eye movement detection methods, including IROG, video-based eye trackers, and SC, the proposed device can measure EOG signals using wet electrodes and classify eight different directions of eye movement relatively easily. The use of wet electrodes ensures that the electrodes remain securely in place on the skin. Our experimental results demonstrate good classification performance, indicating that eye movement detection can be performed reliably. Thus, this EOG-based HCI, designed to detect eight directions of eye movement, will be useful in real-life applications.

ACKNOWLEDGMENT

The authors would like to thank Prof. Li-Wei, Ko, Chun-Wei, Wu, Xen-Ting, Lin, Po- Sheng, Wang, Yu-Ting, Liu, Tsen, Tsai and all members at Brain Research Center, National Chiao Tung University, Taiwan, for their help in preparing and doing the experiment.

REFERENCES

[1] F. Pagnini, "Psychological wellbeing and quality of life in amyotrophic lateral sclerosis: A review," *Int. J. Psychol.*, Jun. 25, 2012.
[2] D. Kruger, "Amyotrophic lateral sclerosis," *J. Amer. Acad. Phys. Assist.*, vol. 25, pp. 53–54, Jul. 2012.
[3] S. Barattelli, L. Sichelschmidt, and G. Rickheit, "Eye-movements as an input in human computer interaction: exploiting natural behaviour," in *Proc. 24th IEEE Annu. Conf. Ind. Electron. Soc.*, 1998, vol. 4, pp. 2000–2005.

[4] J. B. Hiley, A. H. Redekopp, and R. Fazel-Rezai, "A low cost human computer interface based on eye tracking," in *Proc. IEEE Conf. Eng. Med. Biol. Soc.*, 2006, vol. 1, pp. 3226–3229.
[5] M. W. Shen, C. Z. Feng, and H. Su, "Spatial and temporal characteristic of eye movement in human–computer interface design," *Space Med. Med. Eng. (Beijing)*, vol. 16, pp. 304–306, Aug. 2003.
[6] K. U. Schmitt, M. H. Muser, C. Lanz, F. Walz, and U. Schwarz, "Comparing eye movements recorded by search coil and infrared eye tracking," *J. Clin. Monitor. Comput.*, vol. 21, pp. 49–53, Feb. 2007.
[7] M. W. Johns, A. Tucker, J. R. Chapman, E. K. Crowley, and N. Michael, "Monitoring eye and eyelid movements by infrared reflectance oculography to measure drowsiness in drivers," *Somnologie Schlafforschung Schlafmedizin*, vol. 11, pp. 234–242, 2007.
[8] H. D. Crane and C. M. Steele, "Generation-V dual-Purkinje-image eye-tracker," *Appl. Opt.*, vol. 24, pp. 527–537, 1985.
[9] A. Sprenger, B. Neppert, S. Koster, S. Gais, D. Kompf, C. Helmchen, and H. Kimmig, "Long-term eye movement recordings with a scleral search coil-eyelid protection device allows new applications," *J. Neurosci. Methods*, vol. 170, pp. 305–309, May 30, 2008.
[10] M. Lappe-Osthege, S. Talamo, C. Helmchen, and A. Sprenger, "Overestimation of saccadic peak velocity recorded by electro-oculography compared to video-oculography and scleral search coil," *Clin. Neurophysiol.*, vol. 121, pp. 1786–1787, Oct. 2010.
[11] R. Barea, L. Boquete, J. M. Rodriguez-Ascariz, S. Ortega, and E. Lopez, "Sensory system for implementing a human–computer interface based on electrooculography," *Sensors (Basel)*, vol. 11, pp. 310–328, 2011.
[12] W. Heide, E. Koenig, P. Trillenberg, D. Kompf, and D. S. Zee, "Electrooculography: technical standards and applications. The international federation of clinical neurophysiology," *Electroencephalogr. Clin. Neurophysiol. Suppl.*, vol. 52, pp. 223–240, 1999.
[13] P. M. Walter, W. Sickel, K. Gothe, and R. Brunner, "Recording and analysis of the electrooculography using a personal computer. Initial experiences with normal probands and patients with diseases of the posterior eye segment and intraocular foreign bodies," *Klin Monbl Augenheilkd*, vol. 195, pp. 261–267, Oct. 1989.
[14] V. Ciotti, "20 years of HCI," *Healthcare Informat.*, vol. 27, p. 64, Feb. 2010.
[15] J. Gomez-Gil, I. San-Jose-Gonzalez, L. F. Nicolas-Alonso, and S. Alonso-Garcia, "Steering a tractor by means of an EMG-based human-machine interface," *Sensors (Basel)*, vol. 11, pp. 7110–7126, 2011.
[16] I. Mohammad Rezazadeh, S. M. Firoozabadi, H. Hu, and S. M. H. Golpayegani, "A novel human–machine interface based on recognition of multi-channel facial bioelectric signals," *Austral. Phys. Eng. Sci. Med.*, vol. 34, pp. 497–513, Dec. 2011.
[17] L. Y. Deng, C. L. Hsu, T. C. Lin, J. S. Tuan, and S. M. Chang, "EOG-based human–computer interface system development," *Expert Syst. Appl.*, vol. 37, pp. 3337–3343, Apr. 2010.
[18] R. Barea, L. Boquete, M. Mazo, and E. Lpez, "Wheelchair guidance strategies using EOG," *J. Intell. Robot. Syst.*, vol. 34, pp. 279–299, 2002.
[19] H. S. Dhillon, R. Singla, N. S. Rekhi, and R. Jha, "EOG and EMG based virtual keyboard: A brain–computer interface," in *Proc. 2nd IEEE Int. Conf. Comput. Sci. Inf. Technol.*, 2009, pp. 259–262.
[20] J.-C. Chiou, L.-W. Ko, C.-T. Lin, C.-T. Hong, T.-P. Jung, S.-F. Liang, and J.-L. Jeng, "Using novel MEMS EEG sensors in detecting drowsiness application," in *Proc. IEEE Conf. Biomed. Circuits Syst.*, 2006, pp. 33–36.
[21] T. O. A. M. Kawasumi, "Development of an input operation for the amyotrophic lateral sclerosis communication tool utilizing EOG," *Trans. Jpn. Soc. Med. Biol. Eng.*, vol. 43, pp. 172–178, 2005.
[22] J. R. LaCourse and F. C. Hludik, Jr., "An eye movement communication-control system for the disabled," *IEEE Trans. Biomed. Eng.*, vol. 37, no. 12, pp. 1215–1220, Dec. 1990.
[23] A. P. S. Aungsakun, P. Phukpattaranont, and C. Limsakul, "Development of robust EOG-based human–computer interface controlled by eight-directional eye movements," *Int. J. Phys. Sci.*, vol. 7, pp. 2196–2208, Mar. 2012.
[24] Y. Punsawad, Y. Wongsawat, and M. Parnichkun, "Hybrid EEG-EOG brain–computer interface system for practical machine control," in *Proc. IEEE Conf. Eng. Med. Biol. Soc.*, 2010, vol. 2010, pp. 1360–1363.
[25] M. Hazrati and A. Erfanian, "An online EEG-based brain–computer interface for controlling hand grasp using an adaptive probabilistic neural network," *Med. Eng. Phys.*, vol. 32, pp. 730–739, Sep. 2010.
[26] P. Tigges, N. Kathmann, and R. R. Engel, "Identification of input variables for feature based artificial neural networks-saccade detection in EOG recordings," *Int. J. Med. Informat.*, vol. 45, pp. 175–184, Jul. 1997.
[27] S. Hu and G. Zheng, "Driver drowsiness detection with eyelid related parameters by support vector machine," *Expert Syst. Appl.*, vol. 36, pp. 7651–7658, 2009.
[28] C.-L. H. Lawrence, Y. Deng, T.-C. Lin, J.-S. Tuan, and Y.-H. Chen, "EOG-based signal detection and verification for HCI," in *Proc. 2009 Int. Conf. Mach. Learn. Cybern.*, pp. 3342–3348.
[29] A. Jampolsky, E. Tamler, and E. Marg, "Artifacts and normal variations in human ocular electromyography," *AMA Arch. Ophthalmol.*, vol. 61, pp. 402–413, Mar. 1959.
[30] S. Rampp, J. Rachinger, C. Scheller, A. Alfieri, C. Strauss, and J. Prell, "How many electromyography channels do we need for facial nerve monitoring?," *J. Clin. Neurophysiol.*, vol. 29, pp. 226–269, Jun. 2012.
[31] R. T. Al-Kasasbeh, M. S. Shamasin, D. E. Skopin, O. Barbaravi, and V. V. Geppener, "Automated detection of artifacts in electroencephalography signals using a linear prediction model," *Meditsinskaia Tekhnika*, pp. 27–31, 2009.
[32] J. Gale, T. L. Signal, A. L. Garden, and P. H. Gander, "Electroencephalography artifacts in workplace alertness monitoring," *Scand. J. Work Environ. Health*, vol. 33, pp. 148–152, Apr. 2007.
[33] R. L. Schoenfeld, "Common-mode rejection ratio—two definitions," *IEEE Trans. Biomed. Eng.*, vol. BME–17, no. 1, pp. 73–74, Jan. 1970.
[34] R. L. Boylestad and L. Nashelsky, *Electronic Devices and Circuit Theory*, 10th ed. Upper Saddle River, NJ,, USA: Pearson/Prentice-Hall, 2009.
[35] D. A. Neamen, *Microelectronics: Circuit Analysis and Design*, 3rd ed. New York, NY,, USA: McGraw-Hill, 2007.
[36] K. K. Kim, Y. K. Lim, and K. S. Park, "Common mode noise cancellation for electrically non-contact ECG measurement system on a chair," in *Proc. 27th IEEE Annu. Int. Conf. Eng. Med. Biol. Soc.*, 2005, vol. 6, pp. 5881–5883.

Shang-Lin Wu was born in Kaohsiung, Taiwan, in 1987. He received the B.S. and M.S. degrees in the Department of Computer Science and Information Engineering from National Chiayi University, Chiayi, Taiwan, in 2009 and 2011, respectively. He is currently working toward the Ph.D. degree in the Institute of Electrical Control Engineering at National Chiao Tung University (NCTU), Hsinchu, Taiwan.

His research interests are in the areas of biomedical signal processing, biofeedback control, and embedded system.

Lun-De Liao (M'10) received the B.S. degree in mechanical engineering from Chung Yuan Christian University, Taiwan, in 2006, the M.S. degree in engineering science from the National Cheng-Kung University, Taiwan, in 2008, and the Ph.D. degree in electrical engineering from the National Chiao Tung University (NCTU), Taiwan, in 2012.

He was a Research Fellow of the Brain Research Center (BRC) in NCTU. He is currently a Research Scientist in Singapore Institute for Neurotechnology (SINAPSE), National University of Singapore, Singapore. He is an author of *Relativistic Molecular Dynamics Simulation of Ultrafast Laser Ablation*, published by VDM Verlag, Dr. Mller, 2008. He has published over 40 peer-reviewed SCI journal papers and 10 patents. In recent years, his research interests include *in vivo* optical imaging, advanced sensing techniques, brain imaging, and cerebral neuroscience.

Dr. Liao was the recipient of the 2005 Best Paper Award from National Society of Engineers, Taiwan; 2009 SID Travel Fellowship; 2009 IEEE Intermag Travel Fellowship; 2009 the Best Paper Award from the Symposium on NanoDevice Technology; 2010 Honorable Design Award from National Embedded System Design Contest by Ministry of Education; 2010 Best Paper Award from International Symposium on Biomedical Engineering. In 2011, he also won the 1st place of Young Investigator's Awards from the world association for Chinese Biomedical Engineers for his contributions on medical imaging and bioelectronics domain. He was also selected as an Outstanding Research Award of 2012 from National Chiao Tung University, for his outstanding research performance. He currently serves as Co-Editors-in-Chief of the *Journal of Neuroscience and Neuroengineering*, also an Associate Editor of the *Journal of Nanoscience and Nanotechnology* and *Advanced Science, Engineering, and Medicine*.

Shao-Wei Lu was born in Taoyuan, Taiwan, in 1980. He received the B.S. degree from the Department of Physics, National Tsing Hua University, Hsinchu, Taiwan, in 2004 and the Master's degree from the Institute of Molecular Medicine, National Tsing Hua University, in 2007. He is currently working toward the Ph.D. degree in electrical control engineering at National Chiao Tung University, major in physiological signal processing.

His research interests include the information coding of the rabbit retinal ganglion cells.

Wei-Ling Jiang was born in Taiwan, in 1987. He received the B.S. degree from the Department of Electrical Engineering, National Chiao Tung University, Hsinchu, Taiwan, in 2010 and the Master's degree from the Institute of Imaging and Biomedical Photonics, National Chiao Tung University, in 2012.

After graduated, he derived benefit from the knowledge of his research area.

Shi-An Chen (S'09–M'10–S'11–M'12) received the Ph.D. degree in electrical and control engineering from the National Chiao Tung University, Hsinchu, Taiwan, in 2011.

He is currently working in Brain Research Center at National Chiao Tung University, Hsinchu, Taiwan as a Postdoctoral Researcher. His primary research interests are biomedical signal processing, and application of brain computer interaction. Currently, his research focuses on spatial and frequency properties of EEG and cognition state analysis.

Chin-Teng Lin (S'88–M'91–SM'99–F'05) received the B.S. degree in control engineering from the National Chiao-Tung University (NCTU), Hsinchu, Taiwan, in 1986, and the M.S.E.E. and Ph.D. degrees in electrical engineering from Purdue University, West Lafayette, IN, USA, in 1989 and 1992, respectively.

Since August 1992, he has been with the College of Electrical Engineering and the College of Computer Science, NCTU, where he is the Provost and the Lifelong Chair Professor of the Department of Electrical Engineering. He served as the Founding Dean of Computer Science College of NCTU from 2005 to 2007. He is the author of *Neural Fuzzy Systems* (Prentice Hall) and *Neural Fuzzy Control Systems with Structure and Parameter Learning* (World Scientific). He has published over 187 journal papers, including about 77 IEEE TRANSACTION papers. His research interests include translational neuroscience, computational intelligent technologies, soft computing, brain computer interface, smart living technology, intelligent transportation systems, robotics and intelligent sensing, and NBIC (Nano-Bio-Information Technologies and Cognitive science).

Dr. Lin became Fellow of the IEEE for contributions to biologically inspired information systems, and was elevated International Fuzzy Systems Association (IFSA) Fellow in 2012. He was honored with Outstanding Electrical and Computer Engineer (OECE), Purdue University, in 2011. He was a Member of the Board of Governors (BoG) of the IEEE SYSTEMS, MAN, CYBERNETICS SOCIETY (SMCS) from 2003 to 2005, the IEEE Circuit and Systems Society (CASS) (from 2005 to 2008), and the current AdCom member of the IEEE Computational Intelligence Society (CIS) (from 2008 to 2010). He is the IEEE Distinguished Lecturer from 2003 to 2005. He currently serves as an Editor-in-Chief (EIC) of the IEEE TRANSACTIONS ON FUZZY SYSTEMS. He was an Associate Editor of the IEEE TRANSACTIONS ON SYSTEMS, MAN, AND CYBERNETICS, Part II. He also served as the Deputy EIC of the IEEE TRANSACTIONS ON CIRCUITS AND SYSTEMS, Part II from 2006 to 2007. He is the General Chair of the FUZZ-IEEE 2011 held in Taipei, and was the Program Chair of the 2006 IEEE International Conference on Systems, Man, and Cybernetics held in Taipei. He was the President of Board of Government (BoG) of Asia Pacific Neural Networks Assembly (APNNA) from 2004 to 2005. He has won the Outstanding Research Award granted by National Science Council (NSC), Taiwan, since 1997 to present, the Outstanding Professor Award granted by the Chinese Institute of Engineering (CIE) in 2000, and the 2002 Taiwan Outstanding Information-Technology Expert Award. He was also elected to be one of 38th Ten Outstanding Rising Stars in Taiwan (2000). He is a Member of Tau Beta Pi, Eta Kappa Nu and Phi Kappa Phi honorary societies.